

DOI: 10.1002/ange.200501018

**Structural Dualism in the Zwitterionic
7-RR'NH-*nido*-7,8,9-C₃B₈H₁₀ Tricarbollide
Series: An Example of Absolute Tautomerism****

Mario Bakardjiev, Josef Holub, Drahomír Hnyk,
Ivana Císařová, Michael G. S. Londesborough,
Dmitry S. Perekalin, and Bohumil Štíbr*

Tautomerism, which is a dynamic equilibrium between two or more alternative structures of a single species, has been observed for many organic compounds. The commonest case of tautomerism, known as prototropy, is when the electrofuge (a leaving group that does not carry away the bonding electron pair) is a proton. This phenomenon is typical for compounds that contain a functional group that is able to donate a proton, and another functional group which is able to accept it, the functional groups must be in the same molecule and in close enough proximity to one another. The tautomerisation equilibrium is in all cases transmitted by a common anion. The most renowned textbook example of tautomerism is the equilibrium between the keto and enol forms of acetylacetone (Scheme 1).^[1] The tautomerisation constant, defined as $K_T = [\text{enol}]/[\text{keto}]$, is in this case 3.6 for neat acetylacetone.^[1]

Herein we report a unique example of what we would like to term “absolute tautomerism” in the “zwitterionic” tricarbollide series in which a compound adopts one of two different tautomeric forms, either zwitterionic 7-RR'NH-7,8,9-C₃B₈H₁₀ (**Z1**) or neutral 7-RR'N-7,8,9-C₃B₈H₁₁ (**N1**; where R,R' = H or alkyl groups), depending on the properties of the solvent used.

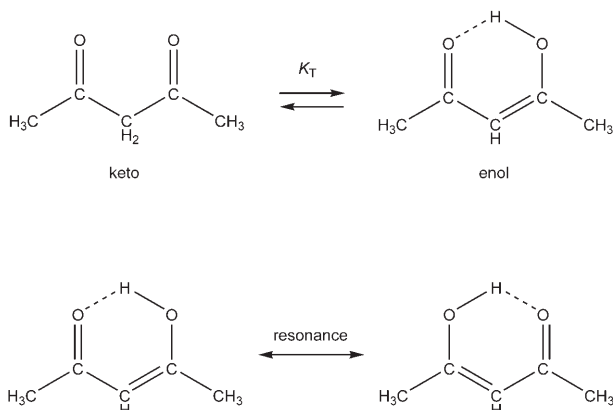
Almost a decade ago we reported the synthesis of the zwitterionic (**Z**) compounds 7-RR'NH-7,8,9-C₃B₈H₁₀ (**Z1**) (where R,R' = H,H (**1a**); H,*t*Bu (**Z1b**); Me,Me (**Z1c**); Me,*t*Bu (**Z1d**)). The NMR spectra for this series in CD₃CN

[*] Dr. M. Bakardjiev, Dr. J. Holub, Dr. D. Hnyk,
Dr. M. G. S. Londesborough, Prof. Dr. B. Štíbr
Institute of Inorganic Chemistry
Academy of Sciences of the Czech Republic
250 68 Řež (Czech Republic)
Fax: (+420) 2-2094-1502
E-mail: stibr@iic.cas.cz

Dr. I. Císařová
Faculty of Natural Sciences of Charles University
Hlavova 2030, 128 42 Prague 2 (Czech Republic)
Fax: (+420) 2-296-084
E-mail: cisarova@natur.cuni.cz

D. S. Perekalin
Institute of Organoelement Compounds
Russian Academy of Sciences
28 ul. Vavilova, 119991, Moscow GSP-1 (Russian Federation)

[**] The work was supported by the Grant Agency of the Czech Republic (project 203/05/2646), Ministry of Education of the Czech Republic (project LC 523), and INTAS project YSF no. 04-83-3848 (to D.S.P.)



Scheme 1. Equilibrium between the tautomeric keto and enol forms of acetylacetone.^[1]

show typical patterns consistent with the structural formulation **Z1**.^[2] Having the zwitterionic character of these compounds in mind, we initially did not attempt NMR spectroscopic measurements in proton nontransferring (PNT) solvents (such as CDCl_3) because of suspected insolubility. Serendipitously, however, we ventured to do so and to our surprise we found that not only are these compounds soluble in CH_2Cl_2 or CHCl_3 , but that their NMR spectra (in CDCl_3) show entirely different NMR patterns (for compounds **N1b** and **Z1b** see Figure 1) that are fully consistent with the

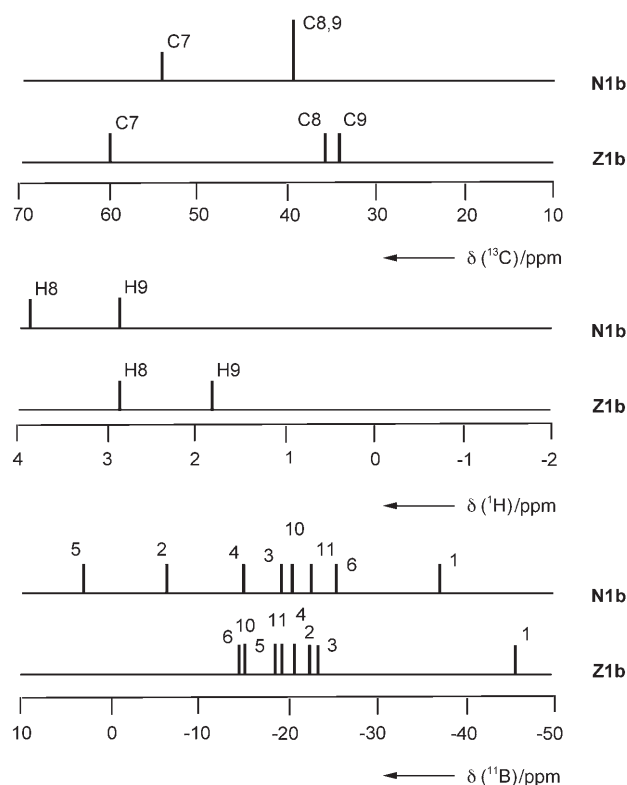
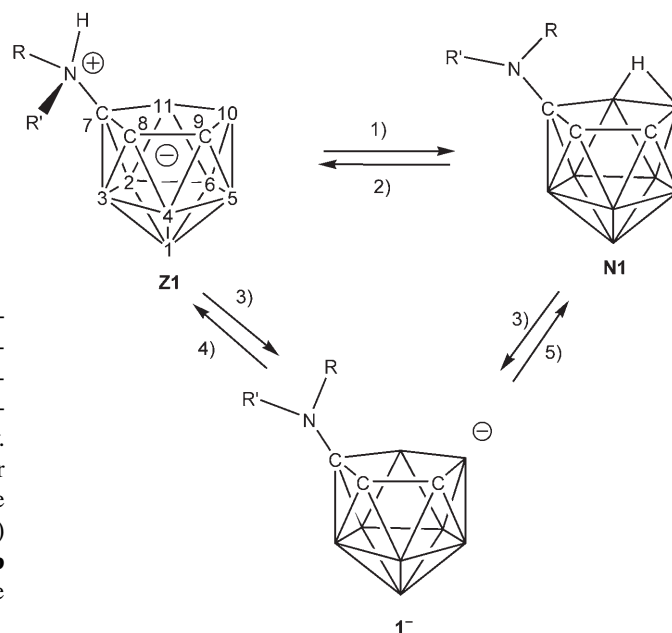


Figure 1. Stick diagrams showing chemical shifts and relative intensities in the ^{11}B (all signals), ^1H (signals from cage CH groups), and ^{13}C NMR (signals cage C atoms) spectra for the tautomeric pair 7-*t*BuNH₂-7,8,9- $\text{C}_3\text{B}_8\text{H}_{10}$ (**Z1b**) and 7-*t*BuNH-7,8,9- $\text{C}_3\text{B}_8\text{H}_{11}$ (**N1b**). For numbering scheme see **Z1** in Scheme 2

neutral tautomeric form of constitution 7-RR'N-7,8,9- $\text{C}_3\text{B}_8\text{H}_{11}$ (**N1**). It should be emphasized that in homogeneous solvent solutions all **Z1**→**N1** conversions are quantitative (at least K_T approaches infinity) with no sign of equilibrium between individual **Z1** and **N1** tautomers detectable in the NMR spectra. As shown in Scheme 2 (path 1) the tautomeric



Scheme 2. The formation and interconversions of the 7-RR'NH-7,8,9- $\text{C}_3\text{B}_8\text{H}_{10}$ (**Z1a**–**Z1d**) and the corresponding 7-RR'N-7,8,9- $\text{C}_3\text{B}_8\text{H}_{11}$ tautomers (**N1a**–**N1d**). 1) dissolution in PNT solvents (such as, CHCl_3 , CH_2Cl_2 , C_6H_6); 2) crystallization from PT solvents (EtOH/water, acetone/water); 3) proton sponge/ CH_2Cl_2 or NaH/ Et_2O ; 4) protonation (H_2SO_4 , CF_3COOH , HCl) in PT solvents; 5) protonation (H_2SO_4 , CF_3COOH , HCl) in PNT solvents. See text for details. C is CH (for C8 and C9), vertices without letters are BH.

conversion is achieved by a simple transfer of an N–H proton to a position bridging B10–B11. Conversely, the **N1** tautomers can also be quantitatively converted into **Z1** tautomers by simple crystallization from proton transferring (PT) solvents (such as EtOH/ H_2O , acetone/ H_2O) or by dissolution in acetonitrile (path 2).

In the case of nonhomogeneous solvent mixtures (see Figure 2) the addition of CH_3CN to a CDCl_3 solution of **N1b** expectedly leads to a classical equilibrium between the **Z1b** and **N1b** tautomers, the equilibrium being defined by the tautomeric constant $K_T = [\text{Z1b}]/[\text{N1b}]$ (where $[\text{Z1b}]$ and $[\text{N1b}]$ are equilibrium concentrations of the zwitterionic and neutral tautomers, respectively). It can be seen from Figure 2 that by adding CH_3CN to a CDCl_3 solution of **N1b** the concentration of the **Z1b** tautomer rapidly grows, and at a CH_3CN volume fraction of approximately 0.25, the **N1b** tautomer disappears from the solution ($[\text{N1b}] = 0$), there are no signals corresponding to the **N1b** tautomer in the ^{11}B and ^1H NMR spectra. This result suggests that at that critical CH_3CN concentration K_T is equal to or approaching infinity.

It is reasonable to suppose that in these tautomeric conversions the proton transfer between the two proton

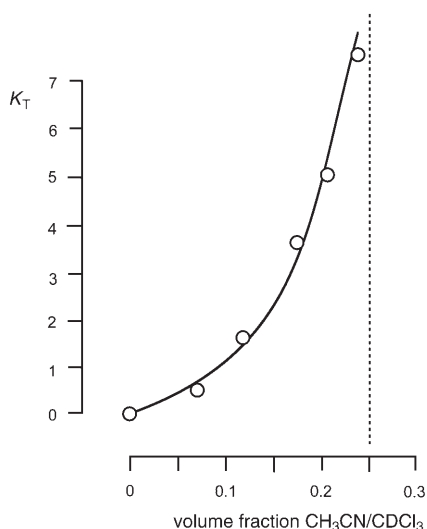


Figure 2. Plot of experimental K_T values versus volume fraction $\text{CH}_3\text{CN}/\text{CDCl}_3$ for the equilibrium between **Z1b** and **N1b** tautomers. At around 0.25 (dotted line) K_T approaches infinity and only one tautomer (**Z1b**) is present in the solution. $K_T = [\text{Z1b}]/[\text{N1b}]$.

accepting centers, the N-atom and the cage B10–B11 bond, occurs through common anions of type $[\text{7-RR}'\text{NH-7,8,9-C}_3\text{B}_8\text{H}_{10}]^-$ (**1**[−]). These anions can be prepared independently by treatment of both tautomers, **Z1** and **N1**, with NaH in Et_2O or proton sponge (PS) in CH_2Cl_2 /hexane mixtures (Scheme 2 (path 3)). Conversely, acidification (HCl, CF_3COOH) of the anions **1**[−] (Na^+ salts) in PT solvents (water, acetonitrile) generates tautomers **Z1** (path 4), while acidification of the PS^+ salts with H_2SO_4 in CH_2Cl_2 leads exclusively to tautomers **N1** (path 5)).

Figure 1 summarizes the NMR patterns for the tautomeric pair **Z1b/N1b**. The remaining compounds from the corresponding **Z1/N1** series exhibit very similar NMR spectroscopic behavior, which we will report elsewhere in a full paper.

The **Z1**-type compounds are derivatives of the $[\text{7,8,9-C}_3\text{B}_8\text{H}_{11}]^-$ ion, while their **N1** tautomers are derivatives of the neutral tricarbolide $\text{7,8,9-C}_3\text{B}_8\text{H}_{12}$.^[2,3] Significant differences between the **Z1** and **N1** tautomers are seen in their ^{11}B NMR spectra, and arise from the presence of the hydrogen atom bridging the B10–B11 bond in **N1**. However, the ^1H and ^{13}C NMR spectra for cage CH and C units are also remarkably different.

The different **Z1** and **N1** tautomers can also be isolated in the solid state. For example, **Z1b** and **N1b** differ in their melting points (148/136°C, respectively) and, moreover, the structure of pure **Z1b** (Figure 3^[4]) and **Z1d**. OCMe_2 ^[2] tautomers were determined by single-crystal X-ray diffraction analysis.

Unfortunately, we have not been able to grow crystals of **N1** compounds, therefore the structures for the simplest tautomeric pair, **Z1a** and **N1a**, were geometrically optimized^[5,6] at the RMP2(fc)/6-31G* level (see Figure 4 and Figure 5). Ignoring variances in H–N–H angles, the main difference (0.094 Å) between them was found for the respective B10–B11 bonds.

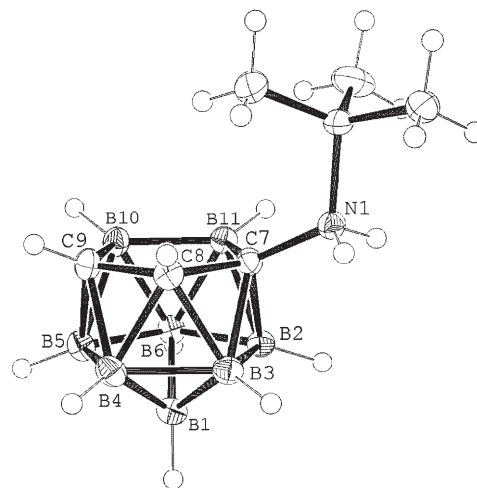


Figure 3. ORTEP representation of the crystallographically determined molecular structure of 7-*t*-BuNH₂-7,8,9- $\text{C}_3\text{B}_8\text{H}_{10}$ (**Z1b**). Selected bond lengths [Å] and angles [°]: B1–B2 1.792(2), B1–B3 1.737(2), B1–B4 1.758(2), B1–B5 1.795(2), B1–B6 1.811(2), B2–B3 1.776(2), B2–B6 1.756(2), B2–C7 1.743(2), B2–B11 1.799(2), B3–B4 1.758(2), B3–C7 1.757(2), B3–C8 1.731(2), B4–B5 1.770(2), B4–C8 1.728(2), B4–C9 1.733(2), B5–B6 1.753(2), B5–C9 1.732(2), B5–B10 1.788(2), B6–B10 1.788(2), B6–B11 1.790(2), C7–C8 1.513(2), C7–B11 1.618(2), C8–C9 1.516(2), C9–B10 1.616(2), B10–B11 1.733(2), N1–C7 1.496(2), N1–C1 1.557(2); B11–C7–C8 112.2(1), C7–C8–C9 110.1(1), C8–C9–B10 110.8(1), C9–B10–B11 104.4(1), C7–B11–B10 102.4(1).

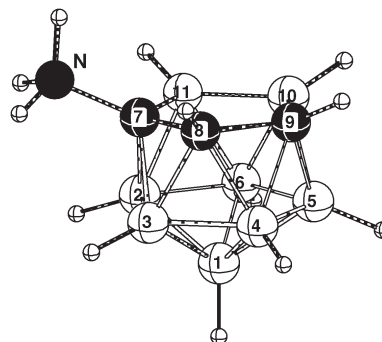


Figure 4. RMP2(fc)/6-31G* optimized geometry of 7-NH₂-7,8,9- $\text{C}_3\text{B}_8\text{H}_{10}$ (**Z1a**). White spheres B, black spheres C. Selected bond lengths [Å] and angles [°]: B1–B2 1.775, B1–B3 1.733, B1–B4 1.761, B1–B5 1.790, B1–B6 1.822, B2–B3 1.779, B2–B6 1.760, B2–C7 1.710, B2–B11 1.804, B3–B4 1.754, B3–C7 1.744, B3–C8 1.739, B4–B5 1.766, B4–C8 1.731, B4–C9 1.737, B5–B6 1.761, B5–C9 1.720, B5–B10 1.788, B6–B10 1.790, B6–B11 1.785, C7–C8 1.508, C7–B11 1.602, C8–C9 1.516, C9–B10 1.625, B10–B11 1.729, C7–N 1.491; C7–C8–C9 108.3, C8–C7–N 117.9, H–N–H (mean) 108.3, H–N–C7 (mean) 110.3. Calculated $\delta(^{11}\text{B})$ chemical shifts (B3LYP/6-31G*//RMP2(fc)/6-31G*) versus experimental (CD_3CN , data from ref. [2]): calcd/exp: B6 –10.8/–15.5, B10 –13.7/–15.5, B11 –19.7/–17.8, B5 –20.8/–18.5, B4 –20.8/–20.2, B2 –23.1/–23.1, B3 –23.8/–23.1, B1 –44.7/–47.1 ppm.

Considering the readiness of interconversion between the **Z1** and **N1** tautomers, a minimal difference in their calculated structure energies might be anticipated. However, the RMP2(fc)/6-31G* calculations on the “free” molecules of **Z1a** and **N1a** in vacuo reveal that the neutral **N1a** tautomer is 22.34 kcal mol^{−1} more stable than **Z1a**. Including the solvent

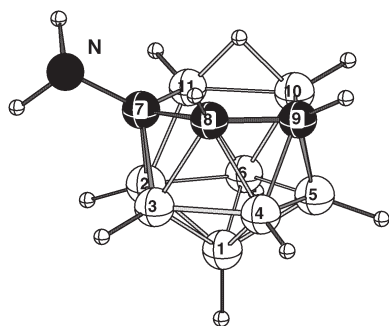


Figure 5. RMP2(fc)/6-31G* optimized geometry of 7-NH₂-7,8,9-C₃B₈H₁₁ (**N1a**). White spheres B, black spheres C. Selected bond lengths [Å] and angles [°]: B1-B2 1.756, B1-B3 1.772, B1-B4 1.777, B1-B5 1.760, B1-B6 1.800, B2-B3 1.753, B2-B6 1.780, B2-C7 1.689, B2-B11 1.796, B3-B4 1.765, B3-C7 1.700, B3-C8 1.720, B4-B5 1.753, B4-C8 1.730, B4-C9 1.695, B5-B6 1.777, B5-C9 1.685, B5-B10 1.804, B6-B10 1.793, B6-B11 1.792, C7-C8 1.532, C7-B11 1.667, C8-C9 1.515, C9-B10 1.657, B10-B11 1.823, C7-N 1.438; C7-C8-C9 116.7, C8-C7-N 115.6, H-N-H (mean) 107.6, H-N-C7 (mean) 110.3, B10-H_b and B11-H_b 1.312. Calculated $\delta(^{11}\text{B})$ chemical shifts (B3LYP/6-31G*/RMP2(fc)/6-31G*) versus experimental (CDCl₃): calcd/exp: B2 3.6/3.9, B5 -5.3/-5.7, B3 -16.9/-16.0, B11 -19.4/-19.5, B4 -21.6/-21.0, B10 -22.2/-22.1, B6 -26.2/-27.0, B1 -35.0/-36.2.

polarity effects in the calculations shows a gradual decrease in the difference between the two tautomers from 6.31 in CHCl₃ to 3.32 in CH₂Cl₂, to 0.15 kcal mol⁻¹ in MeCN. Nevertheless, the experimental observation of a rapid conversion of **N1a** into **Z1a** upon only small polarity change indicates that **Z1a** is stabilized by some specific interaction with acetonitrile (most probably, hydrogen bonding). The mass spectra of both **Z1** and **N1** show essentially the same fragmentation patterns, which indicates that the **Z1**→**N1** conversions proceed under the conditions of the mass-spectrometric experiment.

As far as we are aware, the isolation of pure tautomers of type **1** represents the first example of absolute tautomerism, and thus introduces a new type of structural dualism to chemistry.

Experimental Section

Typical experiments outlined below for compound **1b** are generally applicable to all compounds of constitution **1**.

Z1b: Compounds **Z1b** (102 mg, 0.5 mmol, prepared as reported earlier^[2]) and **N1b** (102 mg, 0.5 mmol) were re-crystallized from a hot EtOH/H₂O mixture to give 100 mg (98%) of **Z1b**. For **Z1b**: For ¹¹B and ¹H NMR spectra see ref. [2] ¹³C NMR (125.8 MHz, CD₃CN, 295 K): δ = 65.0 (s, 1 C, *t*Bu), 60.9 (br, s, 1 C, C7), 35.6 (br, s, 1 C, C8), 34.1 (br, s, 1 C, C9), 27.4 ppm (q, ¹J(C,H) = 129 Hz, 3 C, *t*Bu).

N1b: Compound **Z1b** (205 mg, 1 mmol) was dissolved in CH₂Cl₂ or CHCl₃ (10 mL). Diffusion in of hexane vapors led to crystallization to yield 158 mg (77%) of crystalline **N1b**. Further amount of **N1b** (42 mg, 21%, total yield of **N1b** 98%) was obtained by evaporation of mother liquors. For **N1b**: m.p. 136°C; ¹¹B NMR (128.3 MHz, 25°C, CDCl₃): δ = 2.8 (d, ¹J(B,H) = 159 Hz, 1 B; B2), -6.2 (d, ¹J(B,H) = 162 Hz, 1 B; B5), -15.2 (d, ¹J(B,H) = 171 Hz, 1 B; B3), -19.7 (d, ¹J(B,H) ≈ 170 Hz, 1 B; B4), -20.7 (d, ¹J(B,H) ≈ 140 Hz, 1 B; B11), -22.1 (d, ¹J(B,H) ≈ 150 Hz, 1 B; B10), -25.9 (d, ¹J(B,H) = 150 Hz, 1 B; B6), -37.2 ppm (d, ¹J(B,H) = 152 Hz, 1 B; B1), all theoretical [¹¹B-¹H] cross-peaks are observed; ¹H{¹¹B} NMR (400 MHz, 25°C, CDCl₃): δ = 3.88 (s, 1 H; H8), 3.01 (s, 1 H; H2), 2.73 (s, 1 H; H9), 2.48

(s, 1 H; H5), 2.17 (s, 1 H; H11), 2.00 (s, 1 H; H4), 1.89 (s, 1 H; H3), 1.83 (s, 1 H; H10), 1.1 (s, 2 H; H1, H6), -2.27 ppm (s, 1 H; μ H); ¹³C{¹H} NMR (100.2 MHz, CDCl₃, 295 K): δ = 69.1 (s, 1 C, *t*Bu), 54.9 (br, s, 1 C, C7), 39.2 (br, s, 2 C, C8, C9), 31.1 (s, 3 C, *t*Bu); C₇H₂₁B₈N (205.73): elemental analysis calcd (%) C 40.87, H 10.29; found C 40.64, H 10.12. A solution of PSH⁺**1b**⁻ (50 mg, 0.12 mmol; PS = proton sponge) in CH₂Cl₂ (10 mL) was treated dropwise with concentrated H₂SO₄ (0.5 mL) under cooling and stirring. The CH₂Cl₂ layer was collected, shaken with water (2 × 20 mL), dried over CaCl₂, and evaporated to afford 12 mg (84%) of **N1b**, which was identified by NMR spectroscopy.

1b⁻: A solution of compounds **Z1b** or **N1b** (102 mg, 0.5 mmol) in Et₂O (20 mL) was treated with NaH (ca. 50 mg, 2 mmol) under stirring at room temperature for 12 h. The mixture was then filtered under anaerobic conditions, the filtrate evaporated, and the residual solid dried at room temperature for 24 h to give Na⁺**1b**⁻·OEt₂ (145 mg, 96%) as white crystals. For Na⁺**1b**⁻·OEt₂: m.p. > 350°C (decomp.); ¹¹B NMR (128.3 MHz, 25°C, CD₃CN): δ = -15.4 (d, -, 1 B; B6), -16.8 (d, -, 2 B; B10,11), -17.7 (d, -, 1 B; B5), -18.9 (d, -, 1 B; B4), -23.5 (d, ¹J(B,H) = 161 Hz, 1 B; B3), -25.3 (d, ¹J(B,H) = 146 Hz, 1 B; B2), -48.0 ppm (d, ¹J(B,H) = 138 Hz, 1 B; B1), all theoretical [¹¹B-¹H] cross-peaks observed; - indicates couple constants that could not be determined ¹H{¹¹B} NMR (400 MHz, 25°C, CD₃CN): δ = 3.61 (s, 1 H; NH), 3.39 (t, 2 H; Et₂O), 2.31 (s, 1 H; H9), 1.77 (s, 1 H; H8), 1.45 (s, 1 H; H3), 1.38 (s, 1 H; H4), 1.30 (q, 3 H; Et₂O), 1.29 (s, 1 H; H10 or H11), 1.12 (s, 9 H; *t*Bu), 0.96 (s, 1 H; H5), 0.93 (s, 1 H; H6), 0.92 (s, 1 H; H10 or H11), 0.77 (s, 1 H; H2), -0.16 ppm (s, 1 H; H1); C₁₁H₃₀NB₈ONa (301.83): elemental analysis calcd (%) Na 7.62; found Na 7.56. A solution of compound **N1b** (50 mg, 0.24 mmol) in CH₂Cl₂ (10 mL) was treated with proton sponge (ca. 50 mg, 2 mmol) hexane (20 mL) was carefully layered onto the surface of the solution. After allowing the solution to stand for 24 h, the crystals were isolated by filtration, washed with hexane, and vacuum dried to give 91 mg (90%) of PSH⁺**1b**⁻, which was identified by NMR spectroscopy.

Received: March 21, 2005

Published online: August 11, 2005

Keywords: boron · carboranes · density functional theory · structural dualism · tautomerism

- [1] See, for example: J. D. Roberts, M. C. Caseiro, *Basic Principles of Organic Chemistry*, W. A. Benjamin, New York, 1965, pp. 496–498.
- [2] a) B. Štíbr, J. Holub, F. Teixidor, C. Viñas, *J. Chem. Soc. Chem. Commun.* **1995**, 795–796; B. Štíbr, J. Holub, I. Cířřová, F. Teixidor, C. Viñas, J. Fusek, Z. Plzák, *Inorg. Chem.* **1996**, 35, 3635–3642; b) B. Štíbr, J. Holub, J. Plešek, T. Jelínek, B. Grüner, F. Teixidor, C. Viñas, *J. Organomet. Chem.* **1999**, 582, 282–285.
- [3] J. Holub, B. Štíbr, D. Hnyk, J. Fusek, I. Cířřová, F. Teixidor, C. Viñas, Z. Plzák, P. v. R. Schleyer, *J. Am. Chem. Soc.* **1997**, 119, 7750–7759.
- [4] a) Crystal structure data for C₇H₂₁B₈N (**Z1b**): *M*_r = 205.73, colorless crystal, size 0.45 × 0.40 × 0.05 mm³, monoclinic, space group *P*2₁/*c*, *a* = 9.2840(3), *b* = 10.1030(2), *c* = 13.4830(5) Å, β = 106.544(2)°, *V* = 1212.3 Å³, *T* = 150(2) K, *Z* = 4, ρ_{calcd} = 1.127 Mg m⁻³, Data collected on NoniusKappaCCD four-circle diffractometer (MoK α radiation λ = 0.71073 Å, graphite monochromator); θ_{max} = 27.5°. A total of 16478 reflections were measured, 2771 unique (*R*_{int} = 0.044). Absorption was neglected ($\mu(\text{MoK}\alpha)$ = 0.055 mm⁻¹), GoF on *F*² was 1.045, *R*1 (*I* > 2 σ (*i*)) = 0.043, *wR*2 = 0.129. Largest difference Fourier peak and hole 0.219 and -0.211 e Å⁻³. Refinement used SHELXL97 (G. M. Sheldrick, **1997**). CCDC-266543 contains the supplementary crystallographic data for this paper. These data can be obtained

free of charge from the Cambridge Crystallographic Data Centre via www.ccdc.cam.ac.uk/data_request/cif.

- [5] The calculations used the Gaussian03 program package (ref. [6]) and were performed on a PC (FujitsuSiemens). The structures were optimized first at the RHF/6-31G* level without symmetry restrictions (C_1). Second-derivative analysis, carried out at the same level, determined the nature of the stationary points. The minima were characterized with zero imaginary frequencies. Final optimization at the RMP2/6-31G* included the effect of electron correlation. The calculation of the solvation effects on energy were performed for these geometries at the same level of theory using the PC (personal computer) model. The ^{11}B NMR spectroscopy chemical shifts were calculated at B3LYP/6-31G* level by the GIAO method. The complete data are available from the authors.
- [6] Gaussian03 (Revision B.03), M. J. Frisch, G. W. Trucks, H. B. Schlegel, G. E. Scuseria, M. A. Robb, J. R. Cheeseman, J. A. Montgomery, Jr., T. Vreven, K. N. Kudin, J. C. Burant, J. M. Millam, S. S. Iyengar, J. Tomasi, V. Barone, B. Mennucci, M. Cossi, G. Scalmani, N. Rega, G. A. Petersson, H. Nakatsuji, M. Hada, M. Ehara, K. Toyota, R. Fukuda, J. Hasegawa, M. Ishida, T. Nakajima, Y. Honda, O. Kitao, H. Nakai, M. Klene, X. Li, J. E. Knox, H. P. Hratchian, J. B. Cross, C. Adamo, J. Jaramillo, R. Gomperts, R. E. Stratmann, O. Yazyev, A. J. Austin, R. Cammi, C. Pomelli, J. W. Ochterski, P. Y. Ayala, K. Morokuma, G. A. Voth, P. Salvador, J. J. Dannenberg, V. G. Zakrzewski, S. Dapprich, A. D. Daniels, M. C. Strain, O. Farkas, D. K. Malick, A. D. Rabuck, K. Raghavachari, J. B. Foresman, J. V. Ortiz, Q. Cui, A. G. Baboul, S. Clifford, J. Cioslowski, B. B. Stefanov, G. Liu, A. Liashenko, P. Piskorz, I. Komaromi, R. L. Martin, D. J. Fox, T. Keith, M. A. Al-Laham, C. Y. Peng, A. Nanayakkara, M. Challacombe, P. M. W. Gill, B. Johnson, W. Chen, M. W. Wong, C. Gonzalez, J. A. Pople, Gaussian, Inc., Pittsburgh, PA, **2003**.